



	<b>Experiment title:</b> Structure of SpoIIAA and SpoIIAA-P	<b>Experiment number:</b> LS-1811 LS-1532 LS-1673
<b>Beamline:</b> ID14-1 ID14-2 BM14	<b>Date of experiment:</b> from: 25/09/00 to: 26/09/00 from: 25/09/00 to: 26/09/00 from: 06/05/00 to: 08/05/00	<b>Date of report:</b> 30/08/01
<b>Shifts:</b> 1	<b>Local contact(s):</b> Vivian Stojanoff (ID14-1), Soichi Wakatsuki (ID14-2) Gordon Leonard (BM14)	<i>Received at ESRF:</i>
<b>Names and affiliations of applicants</b> (* indicates experimentalists): P. R. Seavers, R. J. Lewis, J. A. Brannigan, K. H. G. Verschueren, J. P. Turkenburg and A. J. Wilkinson  York Structural Biology Laboratory, Chemistry Department, University of York, Heslington, York, YO10 5DD, UK		

## Report:

A fundamental issue in developmental biology is the mechanism by which a cell of one type divides to produce daughter cells with identical chromosomes but different fates. The asymmetric division, which accompanies sporulation in *Bacillus subtilis*, can be used as a simple model for the establishment of cell type. The resulting unequally sized compartments follow different patterns of gene expression, co-ordinated by a succession of alternative RNA polymerase sigma factors. The activity of the first compartment-specific sigma factor,  $\sigma^F$ , is confined to the forespore, even though  $\sigma^F$  is present in the predivisional cell and partitions to both compartments after asymmetric division.  $\sigma^F$  activity is controlled by an anti-sigma factor, SpoIIAB, a phosphorylatable anti-sigma factor antagonist, SpoIIAA and a phosphatase, SpoIIIE. For  $\sigma^F$  to escape the inhibition of SpoIIAB in the forespore, SpoIIAA must be present in its active, dephosphorylated form.

The phosphorylation state of SpoIIAA is a key determinant in  $\sigma^F$  activity and cell fate. For this reason, the structures of phosphorylated and unphosphorylated SpoIIAA were obtained, in order to examine the extent of conformational change accompanying phosphorylation in this system. Crystals of SpoIIAA from *B. subtilis*

were of poor quality (1) so the homologous SpoIIAA protein from *B. sphaericus* was used for structure determination. The statistics for data collected on various beamlines at the ERSF are given in table 1.

The structure of the unphosphorylated, M86V mutant of SpoIIAA was originally solved by MAD to 2.5Å spacing and was subsequently refined to 1.6Å spacing using a high resolution native data set. This structure was then used as a phasing model to solve the structures of native and phosphorylated SpoIIAA by molecular replacement to 2.7 Å and 1.2 Å spacing, respectively. The refinement statistics for these three structures are given in table 2.

A comparison of the native and phosphorylated SpoIIAA structures shows that there are minimal conformational changes accompanying phosphorylation in this system. This may be explained in terms of the dual role played by SpoIIAB, which is both the kinase that phosphorylates SpoIIAA and the sensor of the phosphorylation signal (2). The comparison of the structures of SpoIIAA and SpoIIAA-P has provided vital insight into the control of compartment-specific gene expression during *Bacillus subtilis* sporulation.

	SpoIIAA (MAD) $\lambda$ 1	SpoIIAA (MAD) $\lambda$ 2	SpoIIAA (MAD) $\lambda$ 3	SpoIIAA (M86V)	SpoIIAA (native)	SpoIIAA-P (native)
Beamline	BM14	BM14	BM14	ID 14.2	ID14.3	ID 14.1
Wavelength ( $\lambda$ )	0.9778	0.9787	0.9184	0.930	0.930	0.934
Resolution (Å)	2.50	2.50	2.50	1.61	2.74	1.16
Space group	P2 <sub>1</sub> 2 <sub>1</sub> 2 <sub>1</sub>	P2 <sub>1</sub> 2 <sub>1</sub> 2 <sub>1</sub>	P2 <sub>1</sub> 2 <sub>1</sub> 2 <sub>1</sub>	P2 <sub>1</sub> 2 <sub>1</sub> 2 <sub>1</sub>	P6 <sub>5</sub> 22	P2 <sub>1</sub> 2 <sub>1</sub> 2 <sub>1</sub>
Completeness (%)	97.0 <sup>a</sup> , 76.7 <sup>b</sup>	96.7 <sup>a</sup> , 75.6 <sup>b</sup>	99.4 <sup>a</sup> , 97.9 <sup>b</sup>	96.4 <sup>a</sup> , 87.1 <sup>b</sup>	99.8 <sup>a</sup> , 99.7 <sup>b</sup>	97.9 <sup>a</sup> , 85.4 <sup>b</sup>
R <sub>merge</sub> (%)	3.5 <sup>a</sup> , 5.8 <sup>b</sup>	3.2 <sup>a</sup> , 5.3 <sup>b</sup>	2.9 <sup>a</sup> , 5.2 <sup>b</sup>	7.6 <sup>a</sup> , 24.0 <sup>b</sup>	7.2 <sup>a</sup> , 34.2 <sup>b</sup>	6.8 <sup>a</sup> , 30.0 <sup>b</sup>
I/ $\sigma$ I	19.2 <sup>a</sup> , 8.6 <sup>b</sup>	19.2 <sup>a</sup> , 6.9 <sup>b</sup>	21.8 <sup>a</sup> , 12.9 <sup>b</sup>	19.8 <sup>a</sup> , 5.4 <sup>b</sup>	23.5 <sup>a</sup> , 5.3 <sup>b</sup>	18.9 <sup>a</sup> , 3.7 <sup>b</sup>

**Table 1: Data**

**collection statistics (<sup>a</sup>for all data, <sup>b</sup>for the highest resolution bin).**

	<b>SpoIIAA (M86V)</b>	<b>SpoIIAA (native)</b>	<b>SpoIIAA-P (native)</b>
<b>R<sub>factor</sub></b>	15.9	25.0	13.2
<b>R<sub>free</sub></b>	21.4	30.2	16.4

Refinement statistics.

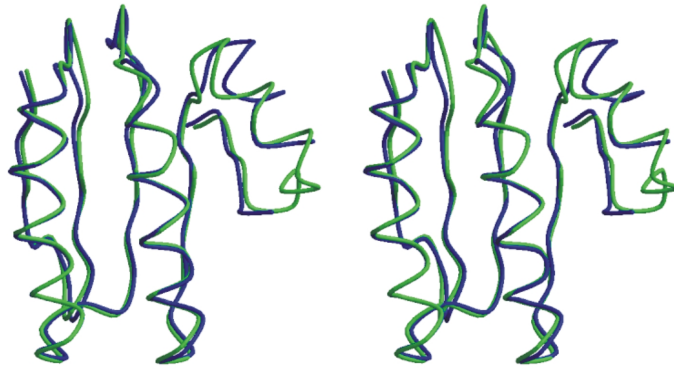


Figure 1:

Comparison between SpoIIAA and SpoIIAA-P from *B. sphaericus*.

- (1) Seavers, P. R., Lewis, R. J., Brannigan, J. A. & Wilkinson, A. J. (2001) *Acta Crystallographica* **D57** 292-295.
- (2) Seavers, P. R., Lewis, R. J., Brannigan, J. A., Verschueren, K. H. G., Murshudov, G. N. & Wilkinson, A. J. (2001) *Structure* **9** 605-614.

